A new acoustic three dimensional intensity and energy density probe

Fabien Ayme, Charles Cariou, Mohamed Ichchou, Daniel Juvé

ACOUSTICS 2012

A new acoustic three dimensional intensity and energy density probe

F. Ayme[a], C. Cariou[b], M. Ichchou[c] and D. Juvé[d]

[a]Ecole Centrale de Lyon, 36,Avenue Guy de Collongue, 69134 Ecully, France
[b]Airbus, 316 route de Bayonne, 31060 Toulouse, France
[c]Laboratoire de Tribologie et Dynamique des Systèmes, 36 Avenue Guy de Collongue, 69134 Ecully Cedex
[d]LMFA Ecole Centrale de Lyon, 36, avenue Guy de Collongue, 69134 Ecully, France
fabien.ayme@ec-lyon.fr

The acoustic field inside aircraft cavities is very complex. Indeed, there is often a combination of direct, diffuse and modal fields depending on the measurement point and on the frequency band considered. This is directly linked to the fact that different types of sources are present. In such cavities, like a cockpit, sources can be panels radiating not necessary in a normal way, avionics systems, air vents, etc...
To find efficient solutions to reduce the noise inside aircraft cavities, a good knowledge of the directivity of the acoustic field in the three dimensions is a great advantage. In this frame, a new intensity acoustic probe has been developed to compute acoustic intensity vector and, acoustic density of energy based on four 1/4" microphones measurements around a small sphere. Its originality consists in the possibility to arrange such probes in an antenna. Several calculation methods have been studied to compute those quantities. Results are compared with intensity measurements of class 1, considered as the reference, in different environments. The probe provides acoustic quantities which can be input data for energetic identification methods.

1 Introduction

Noise matters into aircraft cavities, and especially cockpits have become real subjects of research for the manufacturers which don't only focus on the cabin noise any more. To reduce the internal noise, they need to know how the acoustic field is distributed. But it is also crucial to localize the noise sources, and more important, to obtain a hierarchy of the power injected by those sources. Due to the size of the studied cavity, and the frequency band considered, inverse energetic methods like SEA or MES are appropriate answers to the problem. To retrieve the acoustic power injected into the cavity, they need the active intensity vector and the acoustic density of energy measured on several points. The way to obtain quickly and precisely those quantities into a complex environment is still under investigation.

Indeed, some tools have ever been developed in the past. We can quote for example, Coste [1], who has designed a hard sphere where were integrated six electret microphones, two along the three axis. The university of Brigham [5],[2] has manufactured hard spheres of different diameters, with four or six electret microphones (fig 1a, found in [5]). More recently, in [8], a new hard probe including GRAS 1/4" microphones, and preamplifiers is presented.
Concerning the open spheres, GRAS is selling a one which looks like three unidimensionnal intensity probes, and includes six 1/2" microphones (fig 1b, extracted from [7]). To finish, we can mention the CETIM which has designed an open sphere with four electrostatic 1/4" microphones arranged in a tetrahedron configuration (fig 1c, found in [6]).

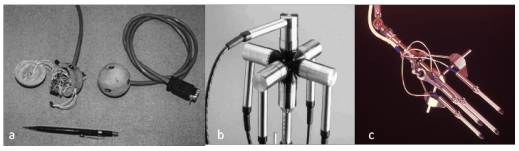

Figure 1: Examples of existing energetic probes

All those probes are not really convenient for providing quickly the acoustic energetic quantities we expect, in all the cavity. Indeed, some of them include electret microphones which are not really stable and accurate, and which are difficult to calibrate quickly and independently [4]. The others integrate microphones of very good quality, but the associated computation method does not take into account the scattering effects created by the microphones on the others.

In this paper, we will propose a new acoustic energetic probe designed to :

- provide results in the frequency band $[350, 5700]Hz$
- integrate 1/4" electrostatic microphones
- use the minimum number of microphones
- include a computation method which implies the minimum error
- be calibrated quickly and accurately
- allow an antenna disposition with several probes
- allow a scanning method of measurement

First, the theoretical aspects to compute the acoustic energetic quantities will be presented. Then, we will define the characteristics of the probe, and all the study that has led to its design. To finish, acoustic tests results carried out with the probe and a reference tool will be presented, analyzed, and compared.

2 Acoustic energetic quantities

2.1 Three dimensional active intensity

The three dimensional active intensity $\boldsymbol{I}_a$ is computed with the acoustic velocity vector $\boldsymbol{V}_0$ and the pressure p_0 expressed on the same point (1).

$$\boldsymbol{I}_a = \frac{1}{2}\Re(p_0 \boldsymbol{V}_0^*) \tag{1}$$

2.2 Acoustic density of energy

The acoustic density of energy W, or ADE, is also obtained with $\boldsymbol{V}_0$ and p_0 (2). It breaks down into two terms : U, the potential acoustic density of energy, and T, the kinetic acoustic density of energy.

$$W = U + T = \frac{|p_0^2|}{4\rho_0 c^2} + \frac{\rho_0}{4}\boldsymbol{V}_0\boldsymbol{V}_0^* \tag{2}$$

We present now two methods associated with acoustic probes which compute $\boldsymbol{V}_0$ and p_0.

2.3 Differential formulation

Pascal & Li have shown in [6] it is possible to "use a systematic approach" to obtain energetic acoustic quantities with finite-sum and finite-difference approximations for four, five, or six-microphones probes. This method is dedicated to the open sphere probes.

One of the objectives of our probe being to use the minimum number of microphones, we are going to focus on the four microphones probes. For them, the sensors are arranged in a tetrahedron configuration. Two configurations are possible. (3) gives the matrix of the microphones coordinates of the tetrahedron probe we will consider, a being the radius of the probe.

$$\mathbf{M} = \begin{bmatrix} \frac{a}{3} & -\frac{2a}{\sqrt{6}} & \frac{a\sqrt{2}}{3} \\ \frac{a}{3} & \frac{2a}{\sqrt{6}} & \frac{a\sqrt{2}}{3} \\ \frac{a}{3} & 0 & -\frac{2a\sqrt{2}}{3} \\ -a & 0 & 0 \end{bmatrix} \tag{3}$$

Then, the formulation of particular velocity resulting in this case is provided by (4).

$$\boldsymbol{V}_0 = \begin{bmatrix} \partial p/\partial x \\ \partial p/\partial y \\ \partial p/\partial z \end{bmatrix} \approx \frac{i}{\rho w.4a} \begin{bmatrix} (3p_4 - p_1 - p_2 - p_3) \\ \sqrt{6}(p_1 - p_2) \\ \sqrt{2}(2p_3 - p_1 - p_2) \end{bmatrix} \tag{4}$$

The pressure p_0 at the center of the probe is obtained by averaging the four pressure measured around the sphere (5).

$$p_0 = \frac{1}{4}(p_1 + p_2 + p_3 + p_4) \tag{5}$$

In [6], Pascal & Li present the errors on the resulting intensity for all the probes as a function of the ka product, from 0 to almost 1.8. The error in high frequencies is directly due to the calculation method. For example, for $ka = 1.6$, the error on the norm of the intensity can reach 2dB, and the angular error almost 10°. The maximum error on the potential energy is almost 2 dB, and 1dB for the kinetic energy. Those errors depend on the incidence of the wave. Here, they are mentioned for the worst cases.
To finish, the error in low frequencies and the phase mismatch are closely related. Indeed, in this frequency domain, the phase mismatch and the phase differences between the microphones can be equivalent.

2.4 Spherical Harmonics formulation

E.G Williams in [10] has developed theoretical aspects of acoustic scattering of plane, and spherical waves around hard spheres. After solving the wave equation in spherical coordinates, the pressure produced by a plane wave can be expressed on a point defined by its spherical coordinates (r, θ, ϕ) with the spherical harmonics (6). p_0 and (θ_i, ϕ_i) are the amplitude, and the incidence of the wave.

$$p_i(r, \theta, \phi, \omega) = 4\pi.p_0 \sum_{n=0}^{\infty} i^n b_n \sum_{m=-n}^{n} Y_n^m(\theta, \phi) Y_n^m(\theta_i, \phi_i)^* \tag{6}$$

In free field $b_n = j_n(kr)$, and in the case of a hard sphere of radius a, $b_n = \left(j_n(kr) - \frac{j_n'(ka)}{h_n'(ka)} h_n(kr)\right)$.

Now, let's focus on the inverse spherical harmonics formulation detailed in [3]. The goal here is to retrieve the amplitude p_0 and the direction (θ_i, ϕ_i) of the plane wave, with four measured pressures. (6) leads to the following formulation (7), where $\boldsymbol{p}$ is the vector containing the four pressures.

$$\boldsymbol{p} = p_0 \mathbf{H}.\boldsymbol{Y}_k^H \tag{7}$$

with $\boldsymbol{Y}_k = \left[Y_0^0(\hat{\boldsymbol{k}}) \;\; Y_1^{-1}(\hat{\boldsymbol{k}}) \;\; Y_1^0(\hat{\boldsymbol{k}}) \;\; Y_1^1(\hat{\boldsymbol{k}}) \;\; \cdots\right]$.

To compute $\boldsymbol{Y}_k^H$, a pseudo-inverse decomposition is used. Numerically, a singular value decomposition is done, and the singular values inferior to 3% are rejected. Then, p_0 can be find with the first term of the solution vector (8).

$$p_0 = \sqrt{4\pi}.\left[(\mathbf{H}^H.\mathbf{H})^{-1}.\mathbf{H}^H\boldsymbol{p}\right]_1^* \tag{8}$$

To finish, the unit vector $\hat{\boldsymbol{k}}$ which gives the direction (θ_i, ϕ_i) of the plane wave can be computed. Thus, the acoustic velocity (9), then the acoustic intensity vector (1), and the ADE (2) are calculated.

$$\boldsymbol{V}_0 = \frac{p_0}{\rho c}.\frac{\boldsymbol{k}}{k} \tag{9}$$

In fact, we don't just need to determine three quantities (p_0, θ_i and ϕ_i), but four : the three coordinates of the unit wave vector $\hat{\boldsymbol{k}}$ which lead to (θ_i and ϕ_i), and p_0. Thus, only the problem of a plane wave can be inverted with a four microphones tetrahedron probe. Indeed, the inverse problem with a spherical acoustic wave introduces another quantity : the distance to the source. This leads to an over-constrained system.

The figure 2 shows the errors (°) on the angles ϕ and θ of the unit vector $\hat{\boldsymbol{k}}$, and on p_0 in magnitude (dB) and phase (°), for $ka = 0.55$ and all the wave incidences.

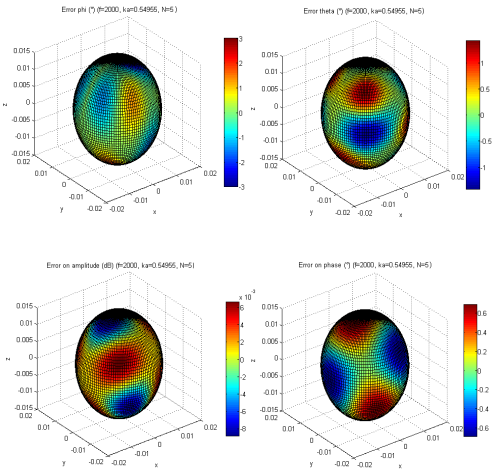

Figure 2: Errors (°) on the angles ϕ and θ, and on the pressure p_0

As can be seen, the errors depend on the incidence of the plane wave, for a same ka. But like for the previous method, the errors are also dependent of ka. In high frequencies they come from the truncation of the harmonics, and from the numerical computation of the pseudo-inverse matrix. They can reach 1.5 dB for ka=1.6. In low frequencies, the errors are very small. Like for the differential method, the low frequencies measurement errors are totally due to phase mismatch. We have limited in this study the range of ka to [0.1;1.6]. It seems to be the best compromise between the more extended frequency band, and the less important errors in low and high frequencies.

3 The acoustic probe

We have seen in the previous section, two methods for obtaining the acoustic energetic quantities, with two kinds of spherical probes. Now, we are going to present our probe, and explain the reasons of our choices.

3.1 Design

Hard spheres avoid scattering matters created by microphones on the others, which are supposed nonexistent for open spheres. Actually, their "'hard characteristic"' creates scattering effects, but which can be taken into account into calculations with a plane wave hypothesis. More-over, hard spheres increase the phase differences between microphones. This is a good effect for low frequencies intensity calculations, as regards to the phase mismatch. Hard spheres provide also a rigid system which is easier for microphones positioning, and allows an antenna configuration. So, the hard sphere configuration gives the possibility to realize more accurate measurements.

Reaching the *ka* range expressed previously, which is a good compromise for the two calculations methods, leads to a radius a of $15mm$ for the frequency band $[350, 5700]$Hz. To realize measurements more punctual around the sphere, and because including four 1/4" microphones is really difficult due to the diameter of the probe, we have decided to connect them behind pipes, integrated into the hard sphere. This kind of measurement has been studied and validated in [12]. To integrate the pipes into the sphere, the decision was taken to limit their curvature. This explains our choice between the two available tetrahedron configurations. Thus, three measurements are done in front of the sphere, and the last one, positioned behind the probe, is done without contact by the last pipe, as shown in figure 3.

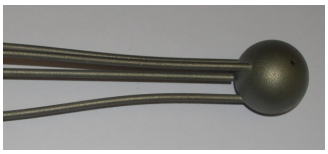

Figure 3: Pipes arrangement around the probe

3.2 Calibration

The calibration of the probe is the key point. It needs to be easy and accurate. Indeed, the connection between the microphone and the pipe creates a standing wave in the tube which has to be taken into account, and corrected with a really accurate transfer function, in amplitude and phase. This function depends on the size of the pipe, the piece which connects the pipe, and the microphone type.

The length of the pipe, and the connection piece play on the amplitude between nodes and antinodes of the function. The interior diameter, and the length of the pipes influence the global level attenuation. More-over, the diameter of the pipes determines the cut-off frequency. To finish, the temperature also influences the calibration function. Due to all those properties, we have made a compromise to design the piece between pipes and microphones, and to fix geometric characteristics of pipes.

In order to simplify the calibration, we have chosen to consider only one length, so only one transfer function for the four pipes. To calibrate the reference pipe, we can use an impedance tube, or a panel in an anechoic room. The two test means provide the same calibration function. The figure 4 shows the calibration technique associated with the panel. As can be seen, the panel is leaky of two holes where a pipe and a reference microphone are introduced flush, separated by 12mm.

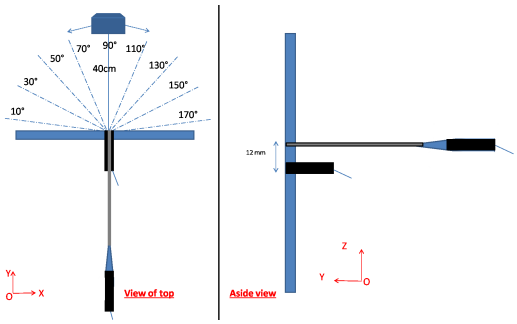

Figure 4: Test device on the panel for the pipe calibration

To judge the quality of the calibration, several tests were carried out. One consisted on measuring the transfer function, then to remove the reference microphone and the tube from the panel, but also the microphone from the pipe. Then, a new transfer function was measured, and the difference with the first one was calculated. The figure 5 shows the result for a single pipe, and two different microphones. The two transfer functions are in good agreement. The differences in amplitude and phase are less than +/-0.5 dB and +/-5° for a normal incidence of the source.

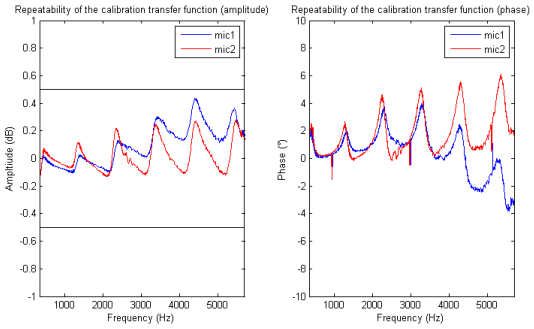

Figure 5: Repeatability of the calibration transfer function

Measurements around the sphere need to be omnidirectional. Thus, the influence of the wave incidence on the calibration has been investigated. Several transfer functions were measured for different incidences from 10° to 170°, as regard to the normal to the panel. This test configuration is represented on the left side of the figure 4. The figure 6 shows the results for four different angles. As can be seen, the transfer function of the pipe is not strictly dependent of the incidence of the acoustic wave. The connection piece between the microphone and the pipe is not the one used now in the final probe. This explains the fairly bad results under

700Hz, where the insulation between the tube and the microphone was deficient. For the final probe, o-rings insure good insulation.

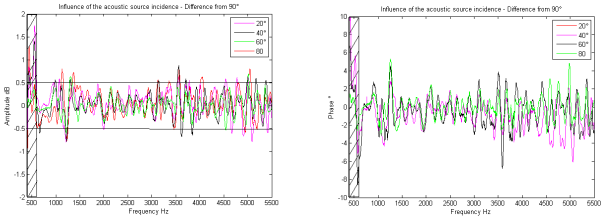

Figure 6: Influence of the acoustic wave incidence on the transfer function

This accuracy of the transfer function can be linked to the class notion of the intensity probe. Here, results could put our probe in, or very close to the class 1 (horizontal lines on fig 6).
The feasibility of the measurement without contact has been demonstrated during tests. More-over, we have also shown that the surface where the pipes flush does not change the previous results (plane or spherical).
All those tests validate the concept of the integration into a sphere of such pipes connected to microphones.

3.3 Calculation methods

As seen before, at least two methods can provide acoustic quantities we are interested in, under different hypothesis. In our case, where measurements will be performed in cavities, with a reactive field, the plane wave hypothesis seems to be inappropriate to obtain the particular velocity. On the other hand, the velocity can't be computed with the differential formulation because our probe is a hard sphere. This is illustrated by the left side of the figure 7.

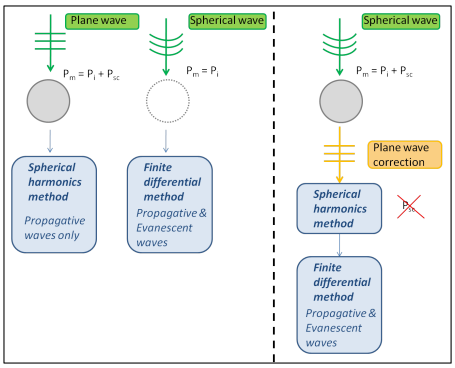

Figure 7: Existing methods of calculation, and a hybrid method

In [11], Elko presents a method to compute the particular velocity with the differential formulation, in the case of a hard sphere. This method is also explained in [5]. As a result, with a small *ka* approximation, for two sensors mounted on a hard sphere, the effect of the sphere consists of artificially increasing the distance between the microphones of a ratio $\frac{3}{2}$.

While Elko applies a correction of first order, assuming $ka \ll 1$, we chose to add the direction and the amplitude of the wave to correct the measured pressures before the velocity calculation. This allows us to remove all the scattered part to the pressure measurements, and then to use after this step four pressures, which are only the result of the incident wave. Our motivation to do that is directly related with the maximum value of ka which is much higher than 1.

The strategy is sum up on the right side of the figure 7. First, the inverse spherical harmonics formulation is used to obtaining the direction of the incident wave and the pressure at the center of the probe. Then, still under a plane wave hypothesis, the scattered part of the pressure on the probe for a plane wave with those characteristics is computed with the direct spherical harmonics formulation. Then, the particular velocity is obtained with the differential formulation from pressures corrected of their scattered part. Those pressures are also averaged to determine the pressure at the center of the probe.

4 Measurements

4.1 Description

Acoustic tests were carried out to evaluate the final probe and the different computation methods. The probe was submitted to different sound fields, from the easier, one source in an anechoic room, to the rougher, two sources in a reverberant room, during punctual or scanning measurements. Moreover, a panel of $640cm^2$ set up between a reverberant and an anechoic room (fig 8), and exciting by a diffuse field has been scanned horizontally by the probe during one minute. The results of this final test are presented below.

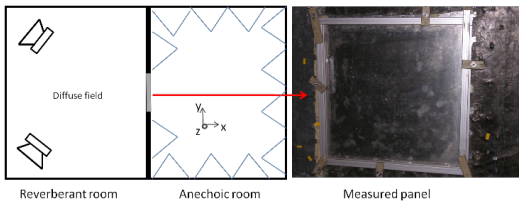

Figure 8: Test in the anechoic room with a panel exciting in the reverberant room

The reference measurement system is a B&K one dimensional intensity probe of class 1. The further results concern the three computation methods:

1. Inverse spherical harmonics method, called later 'harm'
2. Elko's correction of velocity calculation : particular velocity with differential calculations - pressure from inverse spherical harmonics method, called later 'Elko'
3. Complete correction of measured pressures : particular velocity with differential calculations - pressure averaged, called later 'hyb'

4.2 Results

The figure 9 shows the intensity norm, and the density of energy results for the panel scanned by the probe in third octave bands. The reference is here a single normal intensity measurement, because we assume the panel is radiating in a normal way. The 'Elko' method and the reference are in very good agreement from 500Hz to 4000Hz. After, the 'hyb' method seems to be better. We didn't expect the 'Elko' method would provide good results in high frequencies, and the 'hyb' method would underestimate the reference up to 4kHz. As expected, the 'harm' method which does not separate the active field from the reactive one, overestimates the intensity in comparison with the reference.

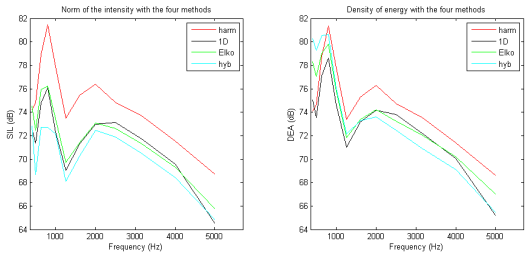

Figure 9: Results on the intensity and the ADE in third octave bands

More-over, as can be seen, the energy density results are fairly good from 1kHz for the 'Elko' method. In analyzing the intensities in the y and z directions, we have noticed a high level for the third octave bands under 1kHz, probably due to leaks on the panel mounting system. This can explain those results.
Thus, the final result of the probe could be the concatenation between the 'Elko' method up to 4 kHz, and the 'hyb' method for the third octave band 5kHz. Several tests carried out in other configurations lead to the same analysis.

5 Conclusion

This article presents a new probe and a strategy for obtaining energetic acoustic quantities. The goal of this work was not to develop a new model of calculation of the energetic acoustic quantities. It was to design a new probe based on existing ones, and meeting some requirements like the possibility to create an antenna, to use 1/4" electrostatical microphones, or to provide same results than a 1D probe, in just one measurement instead of three.

The key point is the integration of pipes connected to the microphones in the hard sphere. This type of measurement allows a calibration of class 1, and it makes possible the design of an antenna of such probes. It is also a good advantage to separate the sphere and the microphones places. Indeed, it will be easier to change a sensor in case of trouble if it is outside the probe, than inside. More-over, the pipes realize very punctual measurements. The smaller the distance between the sensors is, the more punctual the measurements need to be.

Then, the acoustic tests have shown the good behavior of the probe in different kinds of acoustic fields. As regards to the difficulty to perform really accurate tests, the results are really satisfactory. Several tests are in progress to better qualify the acoustic behavior of the probe in different environment. More-over, the way to assemble the probes into a linear antenna, and the association of the probe with an energetic identification method are under investigation.

References

[1] O. Coste, J.C. Patrat, Diffraction autour d'une sphere appliquée a une sonde intensimétrique 3D, 1er congres français d'acoustique (1990), 895-898.

[2] L.L. Locey, Analysis and comparison of three acoustic energy density probes, Master of science, Brigham Young University (2004).

[3] D.C. Thomas, Theory and estimation of acoustic intensity and energy density, Master of science, Brigham Young University (2008).

[4] J.R. Oldham, J.D. Sagers, J.D. Blotter, S.D. Sommerfeldt, T.W. Leishman, K.L. Gee, Development of a multi-microphone calibrator, Applied acoustics 70 (2009), 790-798.

[5] J.W. Parkins, S.D. Sommerfeld, J. Tichy, Error analysis of a pratical energy density sensor, JASA 108 (2000), 211-222.

[6] J.C. Pascal, J.F. Li, A systematic method to obtain 3D finite-difference formulations for acoustic intensity and other enegy quantities, Journal of sound and Vibration 310 (2008), 1093-1111.

[7] GRAS website : http://www.gras.dk/00012/00056/00147/

[8] K.L. Gee, J.H. Giraud, J.D. Blotter, S.D. Sommerfeldt, Near-field vector intensity measurements of a small solid rocket motor, JASA Express Letters 128 (2010), 69-74.

[9] F.J. Fahy, Measurements of acoustic intensity using the cross-spectral density of two microphone signals, JASA 62 (1977), 1057-1059.

[10] E.G Williams, Fourier Acoustics Sound radiation and nearfield acoustical holography, academic Press (1999).

[11] G.W. Elko, An acoustic vector-field probe with calculable obstacle bias, Noise and Vibration Conference (1991), 525-532.

[12] S. Pérennes, Caractérisation des sources de bruit aérodynamique a basses fréquences de dispositifs hypersustentateurs, These de Doctorat, Ecole Centrale de Lyon (1999).